JOURNAL OF AIRCRAFT
Vol. 32, No. 4, July–August 1995

Stability Derivatives for a Hypersonic Caret-Wing Waverider

Christopher Tarpley* and Mark J. Lewis†
University of Maryland, College Park, Maryland 20742

Analytical expressions for the longitudinal and lateral stability derivatives of caret-wing waveriders flying on-design are calculated using linear piston theory. The calculations are extended to off-design conditions with an attached shock wave using tangent wedge theory. The experimental work of Kipke is used to validate the lift and pitch stiffness coefficients. Agreement within 8% is achieved at a Mach number of 7.9 and a Reynolds number of 2.7×10^6. Good agreement is also found with the analytical work done by Hui. The stability derivatives of a Mach 6 waverider are computed, and it is found to have negative pitch and yaw stiffness with the c.g. at the center of volume.

Nomenclature

a = speed of sound, m/s
b = span of planform, m
C_D = drag coefficient, $D/(q_\infty S)$
C_L = lift coefficient, $L/(q_\infty S)$
C_l = rolling moment coefficient about x-body axis, $L/[q_\infty S(b/2)]$
C_m = pitching moment coefficient about y-body axis, $M/[q_\infty S(\bar{c}/2)]$
C_n = yawing moment coefficient about z-body axis, $N/[q_\infty S(b/2)]$
C_X = force coefficient along x-body axis, $X/(q_\infty S)$
C_Y = force coefficient along y-body axis, $Y/(q_\infty S)$
C_Z = force coefficient along z-body axis, $Z/(q_\infty S)$
c = length of topline, m
$\bar{c}$ = mean aerodynamic chord, m
L, M, N = rolling, pitching, and yawing moments, N·m
M_∞ = freestream Mach number
$\boldsymbol{n}$ = surface normal unit vector
p, q, r = perturbation roll, pitch, and yaw rates, rad/s
p^*, q^*, r^* = nondimensional perturbation roll, pitch, and yaw rates, rad $p^* = pb/(2V_\infty)$, $q^* = q\bar{c}/(2V_\infty)$, $r^* = rb/(2V_\infty)$
q_∞ = dynamic pressure, N/m^2
$\boldsymbol{r}$ = surface position vector, m
S = planform area, m^2
T = temperature, K
u, v, w = perturbation velocity components along the body axes, m/s
V = velocity, m/s
X, Y, Z = components of force along the body axes, N
α = angle of attack, rad
β = angle of sideslip or shock wave angle, rad
Γ = angle defining caret-wing, rad
θ = caret-wing wedge angle, rad
Λ = angle defining caret-wing, rad
ρ = density, kg/m^3

Subscripts

l = component on lower surface
lx, ly, lz = lower surface component in x, y, or z direction
p = partial derivative with respect to p^*, $C_{lp} = \partial C_l/\partial p^*$, rad^{-1}
p, q, r = component due to rolling, pitching, or yawing motion
q = partial derivative with respect to q^*, $C_{mq} = \partial C_m/\partial q^*$, rad^{-1}
r = partial derivative with respect to r^*, $C_{lr} = \partial C_l/\partial r^*$, rad^{-1}
u = component on upper surface
u, v, w = component due to u, v, or w motion
ux, uy, uz = upper surface component in x, y, or z direction
$x-w$ = x-direction component due to w motion
$y-w$ = y-direction component due to w motion
$z-w$ = z-direction component due to w motion
α = partial derivative with respect to α, $C_{m\alpha} = \partial C_m/\partial\alpha$, rad^{-1}
β = partial derivative with respect to β, $C_{Y\beta} = \partial C_Y/\partial\beta$, rad^{-1}
0 = on-design angles defining the caret-wing
2 = flow properties behind shock
∞ = freestream flow properties

Presented as Paper 93-0508 at the AIAA 31st Aerospace Sciences Meeting and Exhibit, Reno, NV, Jan. 10–14, 1993; received March 27, 1993; revision received Jan. 26, 1995; accepted for publication Jan. 31, 1995.

*Graduate Research Assistant, Department of Aerospace Engineering. Member AIAA.
†Associate Professor, Department of Aerospace Engineering. Senior Member AIAA.

Introduction

MUCH work has been done on the aerodynamic performance of waveriders. Waverider shape optimization was started by Bowcutt.[1] O'Neill[2] optimized the integration of scramjet engines with the waverider shape, and Takashima[3] used computation fluid dynamics (CFD) to check the off-design performance. The next step towards a practical waverider is inclusion of the stability and control characteristics in the shape optimization. The methodology described here will provide the basis for calculating the stability derivatives of the waverider.

The calculation of stability derivatives requires the analysis of the unsteady flow over the vehicle. Jones[4] and Ribner[5] pioneered this work using potential theory over slender bodies in subsonic and low supersonic flow. Polhamus[6] improved the theory with leading-edge suction to include the effect of the vortex formed by the swept leading edge. Hui[7] has done much work in the area of hypersonic stability. He developed a wedge perturbation theory that has been used in hypersonic flow to compute longitudinal stability derivatives. Liu[8] extended this work to the case of delta wings with attached shocks. A simpler theory called piston theory was proposed by Lighthill[9]

for use in high Mach number flows, $M \geq 4$. Piston theory is based on the idea that in a two-dimensional flow, a perpendicular column of fluid remains intact as it passes over a solid surface. This is because the characteristic lines of the flow are almost parallel to the flow, and so disturbances in the streamwise direction are very small. As a result, the pressure at the solid surface can be calculated as if the surface were a piston moving into a one-dimensional column of fluid.

Piston theory is particularly useful because it equates the disturbance pressure on the surface to the normal surface velocity. As a result, the stability derivatives can be obtained by a single calculation once the steady surface pressure is known. A common alternative is to use a finite difference formulation to calculate the needed derivatives. In the context of an optimization problem, a finite difference requires more function evaluations and may also cause convergence problems for the optimizer.

This article presents a new extension of linear piston theory to the derivation of analytical expressions for the stability derivatives of a specific highlift hypersonic configuration, the caret-wing waverider. Although piston theory is not a new idea, there has been no comprehensive application of piston theory to a derivation such as is done here. These expressions can be used in both the on-design and off-design conditions. A simple modification described by Tarpley and Lewis[10] could extend these piston theory results to supersonic Mach numbers for off-design calculations.

Caret-Wing Geometry

The coordinate system and the geometry of the waverider are shown in Figs. 1 and 2. The vehicle geometry is characterized by the "wedge" angle θ_0 that the undersurface centerline makes with the freestream flow direction. Given the flight Mach number M_∞, the shock angle β_0 is calculated from the $\theta - \beta - M$ relation from oblique shock theory. The leading edge of the caret-wing is chosen to be in the plane of this shock, and so the shock wave is attached to the leading edge. This Mach number is referred to as the "design" Mach number. The body axes are a body-fixed coordinate system with their origin at the c.g. of the vehicle. The x axis is aligned with the upper surface of the caret-wing, which is aligned with the freestream flow of the design condition. The x-z plane is a plane of symmetry of the aircraft. We can calculate the inviscid flow properties on the undersurface exactly from the oblique shock relations. The upper surface is aligned with the freestream and the flow properties there are also known. The angles Λ_0 and Γ_0 define the angles of the upper and lower surface, respectively, and are connected to the vehicle geometry by

$$\tan \Lambda_0 = 2c \tan \beta_0 / b \tag{1}$$

$$\tan \Gamma_0 = b/2c(\tan \beta_0 - \tan \theta_0) \tag{2}$$

The volume of the caret-wing is

$$\text{volume} = bc^2 \tan \theta_0 / 6 \tag{3}$$

The c.g., assuming constant density throughout the volume of the caret-wing, is coincident with the center of the volume, and its position is given by

$$x_{\text{c.g.}}/c = \tfrac{3}{4} \tag{4}$$

$$z_{\text{c.g.}}/c = (\tan \theta_0 + \tan \beta_0)/4 \tag{5}$$

The mean aerodynamic chord is $\bar{c} = \frac{2}{3}c$, and the planform area in the x-y plane is $S = bc/2$.

Analysis

Linear piston theory can be used to estimate the stability derivatives of caret-wing waveriders. On the upper surface,

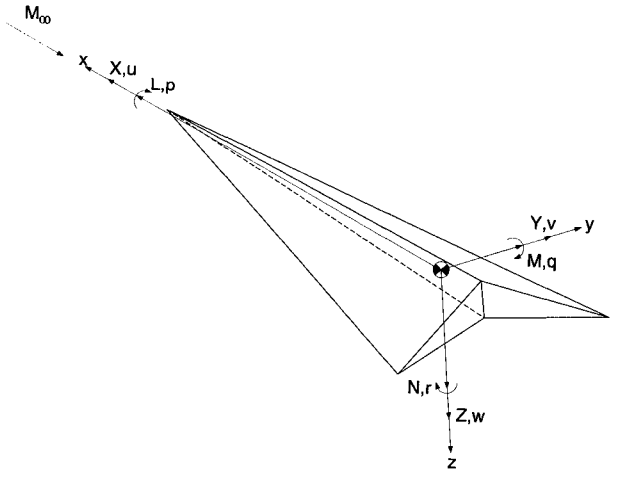

Fig. 1 Caret-wing body fixed coordinate system.

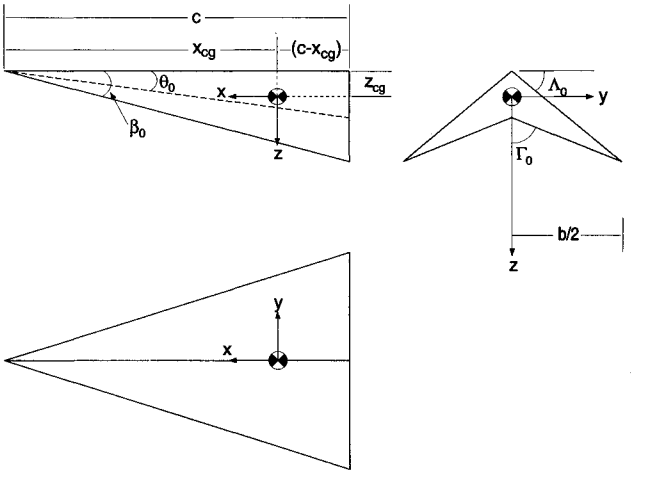

Fig. 2 Caret-wing geometry.

the surface will be modeled as a piston moving into a column of fluid that has the properties of the freestream. On the lower surface, the surface will be modeled as a piston moving into a column of fluid that has the properties of the fluid behind the oblique shock created by the caret-wing. The basic result from linear piston theory is

$$P_{\text{surface}} = P_{\text{steady}} + \rho_{\text{steady}} a_{\text{steady}} V_{\text{surface}} \tag{6}$$

where the subscript "steady" refers to the steady flow conditions past the surface, and V_{surface} refers to the velocity of the surface normal to the steady flow. Equation (6) comes from keeping the first two terms of the binomial expansion of

$$\frac{P_{\text{surface}}}{P_{\text{steady}}} = \left[1 + \frac{\gamma - 1}{2}\left(\frac{V_{\text{surface}}}{a_{\text{steady}}}\right)\right]^{2\gamma/(\gamma-1)} \tag{7}$$

The infinitesimal force due to this pressure is

$$\mathrm{d}\boldsymbol{F} = -P_{\text{surface}}\, \mathrm{d}A\boldsymbol{n} \tag{8}$$

where $\mathrm{d}A$ is the surface element, and $\boldsymbol{n}$ is the outward normal direction.

For the calculation of stability derivatives, we will consider small perturbations from a steady flight condition at M_∞. The perturbations considered will be the velocities u, v, and w

and the rates p, q, and r. The velocity of a point on the upper surface due to these perturbations is

$$\boldsymbol{V}_u = (V_\infty + u)\boldsymbol{i} + v\boldsymbol{j} + w\boldsymbol{k} + \boldsymbol{\omega} \times \boldsymbol{r}_u \tag{9}$$

On the lower surface, we use the flow conditions behind the oblique shock wave. These conditions are calculated with the oblique shock relations. The velocity of a point on the lower surface of the vehicle is

$$\boldsymbol{V}_l = (V_2 \cos\theta_0 + u)\boldsymbol{i} + v\boldsymbol{j} + (w - V_2 \sin\theta_0)\boldsymbol{k} + \boldsymbol{\omega} \times \boldsymbol{r}_l \tag{10}$$

where $\boldsymbol{\omega}$ is the vector $\boldsymbol{\omega} = p\boldsymbol{i} + q\boldsymbol{j} + r\boldsymbol{k}$.

The position of a point on the upper surface is given by the vector

$$\boldsymbol{r}_u = r_{ux}\boldsymbol{i} + r_{uy}\boldsymbol{j} + r_{uz}\boldsymbol{k} \tag{11}$$

with surface normal vector

$$\boldsymbol{n}_u = n_{ux}\boldsymbol{i} + n_{uy}\boldsymbol{j} + n_{uz}\boldsymbol{k} \tag{12}$$

and the lower surface position vector is

$$\boldsymbol{r}_l = r_{lx}\boldsymbol{i} + r_{ly}\boldsymbol{j} + r_{lz}\boldsymbol{k} \tag{13}$$

with surface normal vector

$$\boldsymbol{n}_l = n_{lx}\boldsymbol{i} + n_{ly}\boldsymbol{j} + n_{lz}\boldsymbol{k} \tag{14}$$

By substituting the dot product of Eqs. (9) and (12) into Eq. (6), and then substituting this combined expression into Eq. (8), the infinitesimal force at a point on the upper surface can be written as

$$\begin{aligned}\mathrm{d}\boldsymbol{F}_u = \{&-P_\infty - \rho_\infty a_\infty[(V_\infty + u + r_{uz}q - r_{uy}r)n_{ux} \\ &+ (v + r_{ux}r - r_{uz}p)n_{uy} + (w + r_{uy}p - r_{ux}q)n_{uz}]\}\,\mathrm{d}A_u\boldsymbol{n}_u\end{aligned} \tag{15}$$

Similarly, by substituting the dot product of Eqs. (10) and (14) into Eq. (6), and then substituting this combined expression into Eq. (8), the infinitesimal force at a point on the lower surface can be written as

$$\begin{aligned}\mathrm{d}\boldsymbol{F}_l = \{&-P_2 - \rho_2 a_2[(V_2\cos\theta_0 + u + r_{lz}q - r_{ly}r)n_{lx} \\ &+ (v + r_{lx}r - r_{lz}p)n_{ly} + (w - V_2\sin\theta_0 + r_{ly}p \\ &- r_{lx}q)n_{lz}]\}\,\mathrm{d}A_l\boldsymbol{n}_l\end{aligned} \tag{16}$$

The upper surface element $\mathrm{d}A_u\boldsymbol{n}_u$ can be written as

$$\mathrm{d}A_u\boldsymbol{n}_u = (n_{ux}\boldsymbol{i} + n_{uy}\boldsymbol{j} + n_{uz}\boldsymbol{k})\,\mathrm{d}A_u \tag{17}$$

The lower surface element can be written

$$\mathrm{d}A_l\boldsymbol{n}_l = (n_{lx}\boldsymbol{i} + n_{ly}\boldsymbol{j} + n_{lz}\boldsymbol{k})\,\mathrm{d}A_l \tag{18}$$

Caret-Wing Integration

The previous equations will now be specialized for a caret-wing in the positive y space. Because of the vehicle symmetry, the integrations can be done in the positive y space only. The position vector of a generic point on the upper surface with respect to the c.g. is

$$\begin{aligned}&\boldsymbol{r}_u = x\boldsymbol{i} + y\boldsymbol{j} + (-z_{\text{c.g.}} + y\tan\Lambda_0)\boldsymbol{k} \\ &\text{where } -(c - x_{\text{c.g.}}) \le x \le x_{\text{c.g.}} \\ &0 \le y \le -(b/2c)(x - x_{\text{c.g.}})\end{aligned} \tag{19}$$

the position vector of a generic point on the lower surface with respect to the c.g. is

$$\begin{aligned}&\boldsymbol{r}_l = x\boldsymbol{i} + y\boldsymbol{j} + [-z_{\text{c.g.}} + y\cot\Gamma_0 + (x_{\text{c.g.}} - x)\tan\theta_0]\boldsymbol{k} \\ &\text{where } -(c - x_{\text{c.g.}}) \le x \le x_{\text{c.g.}} \\ &0 \le y \le -(b/2c)(x - x_{\text{c.g.}})\end{aligned} \tag{20}$$

The normal surface vectors are given by

$$\boldsymbol{n}_u = 0\boldsymbol{i} + \sin\Lambda_0\boldsymbol{j} - \cos\Lambda_0\boldsymbol{k} \tag{21}$$

$$\boldsymbol{n}_l = \sin\theta_0\sin\Gamma_0/f\boldsymbol{i} - \cos\theta_0\cos\Gamma_0/f\boldsymbol{j} + \cos\theta_0\sin\Gamma_0/f\boldsymbol{k} \tag{22}$$

where f is

$$f = \sqrt{\sin^2\Gamma_0 + \cos^2\Gamma_0\cos^2\theta_0} \tag{23}$$

When the surface element $\mathrm{d}A\boldsymbol{n}$ is projected onto a plane for performing the integrations, care must be taken with the signs of the differential elements. The transformations that project the surface element onto the various planes are summarized next with the integration limits. Note that on the upper surface n_{ux} is zero:

$$\begin{aligned}&n_{uy}\,\mathrm{d}A_u = \mathrm{d}x\,\mathrm{d}z, \qquad -(c - x_{\text{c.g.}}) \le x \le x_{\text{c.g.}} \\ &-z_{\text{c.g.}} \le z \le -z_{\text{c.g.}} + (x_{\text{c.g.}} - x)\tan\beta_0\end{aligned} \tag{24}$$

$$\begin{aligned}&n_{uz}\,\mathrm{d}A_u = -\mathrm{d}x\,\mathrm{d}y, \qquad -(c - x_{\text{c.g.}}) \le x \le x_{\text{c.g.}} \\ &0 \le y \le -\frac{b}{2c}(x - x_{\text{c.g.}})\end{aligned} \tag{25}$$

$$\begin{aligned}&n_{lx}\,\mathrm{d}A_l = \mathrm{d}y\,\mathrm{d}z, \qquad 0 \le y \le \frac{b}{2}, \qquad -z_{\text{c.g.}} + y\tan\Lambda_0 \\ &\le z \le -z_{\text{c.g.}} + c\tan\theta_0 + y\cot\Gamma_0\end{aligned} \tag{26}$$

$$\begin{aligned}&n_{ly}\,\mathrm{d}A_l = -\mathrm{d}x\,\mathrm{d}z, \qquad -(c - x_{\text{c.g.}}) \le x \le x_{\text{c.g.}} \\ &-z_{\text{c.g.}} + (x_{\text{c.g.}} - x)\tan\theta_0 \le z \le -z_{\text{c.g.}} \\ &+ (x_{\text{c.g.}} - x)\tan\beta_0\end{aligned} \tag{27}$$

$$\begin{aligned}&n_{lz}\,\mathrm{d}A_l = \mathrm{d}x\,\mathrm{d}y, \qquad -(c - x_{\text{c.g.}}) \le x \le x_{\text{c.g.}} \\ &0 \le y \le -\frac{b}{2c}(x - x_{\text{c.g.}})\end{aligned} \tag{28}$$

To calculate the various aerodynamic coefficients, the appropriate pieces of the infinitesimal expressions in Eqs. (15) and (16) are integrated over the surface of the caret-wing. The base pressure is assumed to be P_∞ for the purposes of these calculations, but it only contributes to the C_X and C_m coefficients. Linear piston theory is not used on the rear surface. Note that skin friction is not included in these calculations. The derivatives calculated pertain to step perturbations from straight and level flight.

Z-Force Coefficient: C_Z

The steady Z-force coefficient is calculated by integrating the components of the infinitesimal force expressions related to the steady flow over the surface of the caret-wing. Note that the contribution from the term on the upper surface containing V_∞ disappears because n_{ux} is zero on the upper surface, and the terms containing V_2 on the lower surface cancel each other:

$$\begin{aligned}C_Z &= \frac{1}{q_\infty S}\iint(\mathrm{d}\boldsymbol{F})_{z\text{-steady}} \\ &= \frac{1}{q_\infty S}\left[\iint -P_\infty(n_{uz}\,\mathrm{d}A_u) - \iint P_2(n_{lz}\,\mathrm{d}A_l)\right]\end{aligned} \tag{29}$$

As noted previously, because of the symmetry of the caret-wing, the integration is done in the positive y space only and the integral multiplied by a factor of two. This occurs throughout the remainder of the analysis and will not be mentioned explicitly. The surface differential area is replaced by the corresponding differential area when it is projected into the coordinate plane:

$$C_Z = \frac{2}{q_\infty S}\left[\iint -P_\infty(-\mathrm{d}x\ \mathrm{d}y) - \iint P_2(\mathrm{d}x\ \mathrm{d}y)\right]$$
$$= \frac{-2(P_2 - P_\infty)}{q_\infty S}\int_{-(c-x_{\mathrm{c.g.}})}^{x_{\mathrm{c.g.}}} \mathrm{d}x \int_0^{-(b/2c)(x-x_{\mathrm{c.g.}})} \mathrm{d}y$$
$$= \frac{-4}{\gamma+1}\left(\sin^2\beta_0 - \frac{1}{M_\infty^2}\right) \tag{30}$$

This is a familiar result from two-dimensional oblique shock theory. It is the negative of the pressure coefficient on the lower surface of an infinite plate at angle-of-attack θ_0.

X-Force Coefficient: C_X

The steady X-force coefficient is given by

$$C_X = \frac{1}{q_\infty S}\iint (\mathrm{d}F)_{x\text{-steady}} \tag{31}$$

and for a caret-wing

$$C_X = C_Z \tan\theta_0 \tag{32}$$

In this case, the base pressure has been put into the integration explicitly. The x component of the infinitesimal force on the upper surface is 0.

Lift-to-Drag Ratio: L/D

The inviscid lift-to-drag ratio in the steady flight condition with $\alpha = 0$ is given by $-C_Z/-C_X$, which is equivalent to

$$L/D = \cot\theta_0 \tag{33}$$

Pitch Moment Coefficient: C_m

The steady pitching moment coefficient is given by

$$C_m = \frac{1}{q_\infty S(\bar{c}/2)}\left[\iint z(\mathrm{d}F)_{x\text{-steady}} - \iint x(\mathrm{d}F)_{z\text{-steady}}\right] \tag{34}$$

and for a caret-wing

$$C_m = -C_Z\{3[(x_{\mathrm{c.g.}}/c) - \tfrac{2}{3}] - \tan^2\theta_0$$
$$- \tan\beta_0 \tan\theta_0 + 3\tan\theta_0(z_{\mathrm{c.g.}}/c)\} \tag{35}$$

In this case, the base pressure has also been put into the integration explicitly. The x component of the infinitesimal force on the upper surface is 0.

α Derivative of Z-Force Coefficient: $C_{Z\alpha}$

The change in the Z-force coefficient due to a change in angle of attack is calculated by integrating the component of the infinitesimal force expression that contains the vertical velocity perturbation w:

$$(C_Z)_w = \frac{1}{q_\infty S}\iint (\mathrm{d}F)_{z-w}$$
$$= \frac{1}{q_\infty S}\left[\iint -\rho_\infty a_\infty n_{uz} w(n_{uz}\ \mathrm{d}A_u)\right.$$
$$\left. - \iint \rho_2 a_2 n_{lz} w(n_{lz}\ \mathrm{d}A_l)\right] \tag{36}$$

For a caret-wing

$$(C_Z)_w = \frac{2}{q_\infty S}\iint (\rho_\infty a_\infty n_{uz} - \rho_2 a_2 n_{lz}) w\ \mathrm{d}x\ \mathrm{d}y \tag{37}$$

If $w/V_\infty \ll 1$, then $w/V_\infty \cong \alpha$, and the previous equation can be written

$$(C_Z)_w = \frac{2}{q_\infty S}\iint (\rho_\infty a_\infty n_{uz} - \rho_2 a_2 n_{lz}) V_\infty \alpha\ \mathrm{d}x\ \mathrm{d}y \tag{38}$$

and so

$$\frac{\partial C_Z}{\partial\alpha} = \frac{2}{q_\infty S}\iint (\rho_\infty a_\infty n_{uz} - \rho_2 a_2 n_{lz}) V_\infty\ \mathrm{d}x\ \mathrm{d}y \tag{39}$$

This integral yields

$$\frac{\partial C_Z}{\partial\alpha} = \frac{2}{M_\infty}\left(n_{uz} - \frac{\rho_2}{\rho_\infty}\sqrt{\frac{T_2}{T_\infty}}\, n_{lz}\right) \tag{40}$$

α Derivative of X-Force Coefficient: $C_{X\alpha}$

The change in the X-force coefficient due to a change in angle of attack is calculated from

$$(C_X)_w = \frac{1}{q_\infty S}\iint (\mathrm{d}F)_{x-w} \tag{41}$$

It can also be obtained directly by differentiating the expression for C_X with respect to α to get

$$\frac{\partial C_X}{\partial\alpha} = \frac{2}{M_\infty}\left(n_{uz} - \frac{\rho_2}{\rho_\infty}\sqrt{\frac{T_2}{T_\infty}}\, n_{lz}\right)\tan\theta_0 \tag{42}$$

α Derivative of Pitch Moment Coefficient: $C_{m\alpha}$

The change in pitch moment coefficient due to a change in angle of attack can be calculated from the contribution of the forces due to a velocity w in the z direction:

$$(C_m)_w = \frac{1}{q_\infty S(\bar{c}/2)}\left[\iint z(\mathrm{d}F)_{x-w} - \iint x(\mathrm{d}F)_{z-w}\right]$$
$$= \frac{1}{q_\infty S(\bar{c}/2)}\left\{-\iint z\rho_2 a_2 w n_{lz}(n_{lx}\ \mathrm{d}A_l)\right.$$
$$\left. - \iint x[-\rho_\infty a_\infty w n_{uz}(n_{uz}\ \mathrm{d}A_u) - \rho_2 a_2 w n_{lz}(n_{lz}\ \mathrm{d}A_l)]\right\} \tag{43}$$

The detail will be left out for the rest of the derivatives. Only the base expression and the integration result will be quoted. For a caret-wing

$$\frac{\partial C_m}{\partial\alpha} = -\frac{\rho_2}{\rho_\infty}\sqrt{\frac{T_2}{T_\infty}}\frac{6n_{lz}}{M_\infty}\left[\left(\frac{2}{3} - \frac{x_{\mathrm{c.g.}}}{c}\right)\right.$$
$$\left. - \tan\theta_0\left(\frac{z_{\mathrm{c.g.}}}{c} - \frac{\tan\beta_0 + \tan\theta_0}{3}\right)\right]$$
$$+ \frac{6n_{uz}}{M_\infty}\left(\frac{2}{3} - \frac{x_{\mathrm{c.g.}}}{c}\right) \tag{44}$$

q^* Derivative of Z-Force Coefficient: C_{Zq}

If the caret-wing undergoes a pitching motion about its c.g., the velocity of the surface due to this motion will give rise to

a change in the surface pressure according to piston theory. The Z-force coefficient due to a pitching motion is

$$(C_Z)_q = \frac{1}{q_\infty S}\iint (\mathrm{d}\boldsymbol{F})_{z-q}$$
$$= \frac{1}{q_\infty S}\left[\iint \rho_\infty a_\infty r_{ux} n_{uz}(n_{uz}\,\mathrm{d}A_u) - \iint \rho_2 a_2 (r_{lz}n_{lx} - r_{lx}n_{lz})(n_{lz}\,\mathrm{d}A_l)\right] q \quad (45)$$

and for a caret-wing integrating this gives the expression

$$\frac{\partial C_Z}{\partial(q\bar{c}/2V_\infty)} = -\frac{\rho_2}{\rho_\infty}\sqrt{\frac{T_2}{T_\infty}}\frac{n_{lx}}{M_\infty}\left(2\tan\beta_0 + 2\tan\theta_0 - 6\frac{z_{c.g.}}{c}\right) + 6\left[\frac{\rho_2}{\rho_\infty}\sqrt{\frac{T_2}{T_\infty}}\frac{n_{lz}}{M_\infty} - \frac{n_{uz}}{M_\infty}\right]\left(\frac{x_{c.g.}}{c} - \frac{2}{3}\right) \quad (46)$$

q^* Derivative of Pitch Moment Coefficient: C_{mq}

If a caret-wing undergoes a pitching motion, there will be an induced pressure component on the surface due to the pitch rate q. This moment perturbation can be calculated from

$$(C_m)_q = \frac{1}{q_\infty S(\bar{c}/2)}\left[\iint z(\mathrm{d}\boldsymbol{F})_{x-q} - \iint x(\mathrm{d}\boldsymbol{F})_{z-q}\right]$$
$$= \frac{1}{q_\infty S(\bar{c}/2)}\left[\iint -z\rho_2 a_2(r_{lz}n_{lx} - r_{lx}n_{lz})(n_{lx}\,\mathrm{d}A_l) - \iint x\rho_\infty a_\infty r_{ux}n_{uz}(n_{uz}\,\mathrm{d}A_u) + \iint x\rho_2 a_2(r_{lz}n_{lx} - r_{lx}n_{lz})(n_{lz}\,\mathrm{d}A_l)\right] q \quad (47)$$

For a caret-wing integrating this gives a polynomial in $(x_{c.g.}/c)$, and $(z_{c.g.}/c)$:

$$\frac{\partial C_m}{\partial(q\bar{c}/2V_\infty)} = A + B\frac{x_{c.g.}}{c} + C\left(\frac{x_{c.g.}}{c}\right)^2 + D\frac{z_{c.g.}}{c} + E\left(\frac{z_{c.g.}}{c}\right)^2 + F\frac{x_{c.g.}z_{c.g.}}{c^2} \quad (48)$$

where

$$A = -9\left(a_1 - a_3 + a_2\frac{\tan\beta_0}{2} + a_2\frac{\tan\theta_0}{2} + a_1\frac{\tan\beta_0\tan\theta_0}{2} + a_2\frac{\tan^2\beta_0\tan\theta_0}{3} + a_1\frac{\tan^2\theta_0}{2} + a_2\frac{\tan\beta_0\tan\theta_0^2}{3} + a_2\frac{\tan^3\theta_0}{3}\right) \quad (49)$$

$$B = 24\left(a_1 - a_3 + a_2\frac{\tan\beta_0}{4} + a_2\frac{\tan\theta_0}{4} + a_1\frac{\tan\beta_0\tan\theta_0}{4} + a_1\frac{\tan^2\theta_0}{4}\right) \quad (50)$$

$$C = -18(a_1 - a_3) \quad (51)$$

$$D = 12(a_2 + a_1\tan\theta_0 + a_2\tan\beta_0\tan\theta_0 + a_2\tan^2\theta_0) \quad (52)$$

$$E = -18a_2\tan\theta_0 \quad (53)$$

$$F = -18(a_1\tan\theta_0 + a_2) \quad (54)$$

$$a_1 = (\rho_2/\rho_\infty)\sqrt{(T_2/T_\infty)}(n_{lz}/M_\infty) \quad (55)$$

$$a_2 = (\rho_2/\rho_\infty)\sqrt{(T_2/T_\infty)}(n_{lx}/M_\infty) \quad (56)$$

$$a_3 = n_{uz}/M_\infty \quad (57)$$

β Derivative of Side Force Coefficient: $C_{Y\beta}$

If the caret-wing experiences a velocity in the y direction, it will experience a side force that can be calculated from

$$(C_Y)_v = \frac{1}{q_\infty S}\iint (\mathrm{d}\boldsymbol{F})_{y-v} \quad (58)$$

Performing the integration gives

$$\frac{\partial C_Y}{\partial\beta} = \frac{-4c}{b}\left[\frac{n_{uy}\tan\beta_0}{M_\infty} - \frac{\rho_2}{\rho_\infty}\sqrt{\frac{T_2}{T_\infty}}\frac{n_{ly}}{M_\infty}(\tan\beta_0 - \tan\theta_0)\right] \quad (59)$$

We have used the fact here that if $(v/V_\infty) \ll 1$, then $(v/V_\infty) \cong \beta$.

β Derivative of Roll Moment Coefficient: $C_{l\beta}$

The caret-wing will experience a rolling moment in response to a velocity in the y direction. The moment perturbation can be calculated from

$$(C_l)_v = \frac{1}{q_\infty S(b/2)}\left[\iint y(\mathrm{d}\boldsymbol{F})_{z-v} - \iint z(\mathrm{d}\boldsymbol{F})_{y-v}\right] \quad (60)$$

Carrying out the integration yields

$$\frac{\partial C_l}{\partial\beta} = \frac{2}{3}\left(\frac{n_{uy}}{M_\infty} - \frac{\rho_2}{\rho_\infty}\sqrt{\frac{T_2}{T_\infty}}\frac{n_{ly}}{M_\infty}\right) + \frac{8c^2\tan\beta_0 n_{uy}}{3b^2M_\infty}\left(\tan\beta_0 - 3\frac{z_{c.g.}}{c}\right) + \frac{\rho_2}{\rho_\infty}\sqrt{\frac{T_2}{T_\infty}}\frac{8c^2(-\tan\beta_0 + \tan\theta_0)n_{ly}}{3b^2M_\infty} \times \left(\tan\beta_0 + \tan\theta_0 - 3\frac{z_{c.g.}}{c}\right) \quad (61)$$

β Derivative of Yaw Moment Coefficient: $C_{n\beta}$

The caret-wing will experience a yawing moment in response to a velocity in the y direction that can be calculated from

$$(C_n)_v = \frac{1}{q_\infty S(b/2)}\left[\iint x(\mathrm{d}\boldsymbol{F})_{y-v} - \iint y(\mathrm{d}\boldsymbol{F})_{x-v}\right] \quad (62)$$

Integrating this expression gives

$$\frac{\partial C_n}{\partial\beta} = \frac{n_{uy}}{M_\infty}\frac{8c^2\tan\beta_0}{b^2}\left(\frac{2}{3} - \frac{x_{c.g.}}{c}\right) + \frac{\rho_2}{\rho_\infty}\sqrt{\frac{T_2}{T_\infty}}\frac{n_{ly}}{M_\infty} \times \left[\frac{2}{3}\tan\theta_0 + \frac{8c^2}{b^2}(-\tan\beta_0 + \tan\theta_0)\left(\frac{2}{3} - \frac{x_{c.g.}}{c}\right)\right] \quad (63)$$

This is the weathercock stability derivative.

p^* Derivative of Side Force Coefficient: C_{Y_p}

The side force generated by a rolling motion is given by

$$(C_Y)_p = \frac{1}{q_\infty S}\iint (\mathrm{d}\boldsymbol{F})_{y-p} \tag{64}$$

Integrating this yields

$$\frac{\partial C_Y}{\partial(pb/2V_\infty)} = \frac{4c^2 \tan\beta_0}{3b^2M_\infty}\left(2n_{u_y}\tan\beta_0 - 6n_{u_y}\frac{z_{c.g.}}{c} - \frac{b}{c}n_{u_z}\right)$$
$$+ \frac{\rho_2}{\rho_\infty}\sqrt{\frac{T_2}{T_\infty}}\frac{4c^2(\tan\beta_0 - \tan\theta_0)}{3b^2M_\infty}$$
$$\times\left[\frac{b}{c}n_{l_z} - 2n_{l_y}(\tan\beta_0 + \tan\theta_0) + 6n_{l_y}\frac{z_{c.g.}}{c}\right] \tag{65}$$

p^* Derivative of Roll Moment Coefficient: C_{l_p}

The damping-in-roll moment can be calculated from

$$(C_l)_p = \frac{1}{q_\infty S(b/2)}\left[\iint y(\mathrm{d}\boldsymbol{F})_{z-p} - \iint z(\mathrm{d}\boldsymbol{F})_{y-p}\right] \tag{66}$$

Integrating this gives

$$\frac{\partial C_l}{\partial(pb/2V_\infty)} = \frac{-1}{3M_\infty}\left[\frac{48c^3n_{u_y}\tan\beta_0}{b^3}\left(\frac{z_{c.g.}}{c}\right)^2\right.$$
$$-\left(\frac{4cn_{u_y}}{b} - \frac{8c^2n_{u_z}\tan\beta_0}{b^2} + \frac{32c^3n_{u_y}\tan^2\beta_0}{b^3}\right)\left(\frac{z_{c.g.}}{c}\right)$$
$$\left.-n_{u_z} + \frac{2cn_{u_y}\tan\beta_0}{b} - \frac{4c^2n_{u_z}\tan^2\beta_0}{b^2} + \frac{8c^3n_{u_y}\tan^3\beta_0}{b^3}\right]$$
$$-\frac{\rho_2}{\rho_\infty}\sqrt{\frac{T_2}{T_\infty}}\frac{1}{M_\infty}\left(\frac{n_{l_z}}{3} - \frac{2cn_{l_y}\tan\beta_0}{3b}\right.$$
$$\left.-\frac{cn_{l_y}\tan\theta_0}{3b} + \frac{4cn_{l_y}z_{c.g.}}{3bc}\right) - \frac{\rho_2}{\rho_\infty}\sqrt{\frac{T_2}{T_\infty}}\frac{2c}{3bM_\infty}$$
$$\times(\tan\beta_0 - \tan\theta_0)\left\{\frac{-24c^2n_{l_y}}{b^2}\left(\frac{z_{c.g.}}{c}\right)^2\right.$$
$$-\left[\frac{4cn_{l_z}}{b} - \frac{16c^2n_{l_y}(\tan\beta_0 + \tan\theta_0)}{b^2}\right]\left(\frac{z_{c.g.}}{c}\right)$$
$$+\frac{2cn_{l_z}\tan\beta_0}{b} - \frac{4c^2n_{l_y}\tan^2\beta_0}{b^2} + \frac{cn_{l_z}\tan\theta_0}{b}$$
$$\left.-\frac{4c^2n_{l_y}\tan\theta_0\tan\beta_0}{b^2} - \frac{4c^2n_{l_y}\tan^2\theta_0}{b^2}\right\} \tag{67}$$

p^* Derivative of Yaw Moment Coefficient: C_{n_p}

C_{n_p} is an example of the cross coupling that occurs in the lateral motion between yawing and rolling motions. It can be calculated from

$$(C_n)_p = \frac{1}{q_\infty S(b/2)}\left[\iint x(\mathrm{d}\boldsymbol{F})_{y-p} - \iint y(\mathrm{d}\boldsymbol{F})_{x-p}\right] \tag{68}$$

Integrating this yields

$$\frac{\partial C_n}{\partial(pb/2V_\infty)} = \frac{\rho_2}{\rho_\infty}\sqrt{\frac{T_2}{T_\infty}}\frac{1}{M_\infty}\left[\frac{\tan\theta_0}{3}\left(n_{l_z} - \frac{2cn_{l_y}\tan\beta_0}{b}\right.\right.$$
$$\left.-\frac{cn_{l_y}\tan\theta_0}{b} + \frac{4cn_{l_y}}{b}\frac{z_{c.g.}}{c}\right) - \frac{2c^2(\tan\beta_0 - \tan\theta_0)}{3b^2}$$
$$\times\left(3n_{l_z} - \frac{6cn_{l_y}\tan\beta_0}{b} - \frac{6cn_{l_y}\tan\theta_0}{b} - 4n_{l_z}\frac{x_{c.g.}}{c}\right.$$
$$+\frac{8cn_{l_y}\tan\beta_0}{b}\frac{x_{c.g.}}{c} + \frac{8cn_{l_y}\tan\theta_0}{b}\frac{x_{c.g.}}{c}$$
$$\left.\left.+\frac{16cn_{l_y}}{b}\frac{z_{c.g.}}{c} - \frac{24cn_{l_y}}{b}\frac{x_{c.g.}}{c}\frac{z_{c.g.}}{c}\right)\right] - \frac{2c^2\tan\beta_0}{3b^2M_\infty}$$
$$\times\left(-3n_{u_z} + \frac{6cn_{u_y}\tan\beta_0}{b} + 4n_{u_z}\frac{x_{c.g.}}{c}\right.$$
$$\left.-\frac{8cn_{u_y}\tan\beta_0}{b}\frac{x_{c.g.}}{c} - \frac{16cn_{u_y}}{b}\frac{z_{c.g.}}{c} + \frac{24cn_{u_y}}{b}\frac{x_{c.g.}}{c}\frac{z_{c.g.}}{c}\right) \tag{69}$$

r^* Derivative of Side Force Coefficient: C_{Y_r}

The side force generated by a yawing motion is given by

$$(C_Y)_r = \frac{1}{q_\infty S}\iint (\mathrm{d}\boldsymbol{F})_{y-r} \tag{70}$$

Integrating this gives the expression

$$\frac{\partial C_Y}{\partial(rb/4V_\infty)} = \frac{8c^2n_{u_y}\tan\beta_0}{b^2M_\infty}\left(\frac{2}{3} - \frac{x_{c.g.}}{c}\right) - \frac{\rho_2}{\rho_\infty}\sqrt{\frac{T_2}{T_\infty}}\frac{4c}{3bM_\infty}$$
$$\times\left\{(\tan\beta_0 - \tan\theta_0)\left[n_{l_x} + \frac{6cn_{l_y}}{b}\left(\frac{2}{3} - \frac{x_{c.g.}}{c}\right)\right]\right\} \tag{71}$$

r^* Derivative of Roll Moment Coefficient: C_{l_r}

C_{l_r} is another example of the cross coupling between yawing and rolling motion. It is calculated from

$$(C_l)_r = \frac{1}{q_\infty S(b/2)}\left[\iint y(\mathrm{d}\boldsymbol{F})_{z-r} - \iint z(\mathrm{d}\boldsymbol{F})_{y-r}\right] \tag{72}$$

Integrating this yields

$$\frac{\partial C_l}{\partial(rb/2V_\infty)} = \frac{-4cn_{u_y}}{3bM_\infty}\left[\frac{3}{4} - \frac{x_{c.g.}}{c} + \frac{c^2\tan\beta_0}{b^2}\right.$$
$$\left.\times\left(3\tan\beta_0 - 4\tan\beta_0\frac{x_{c.g.}}{c} - 8\frac{z_{c.g.}}{c} + 12\frac{z_{c.g.}}{c}\frac{x_{c.g.}}{c}\right)\right]$$
$$+\frac{\rho_2}{\rho_\infty}\sqrt{\frac{T_2}{T_\infty}}\frac{1}{M_\infty}\left[\frac{n_{l_x}}{3} + \frac{cn_{l_y}}{b} - \frac{4cn_{l_y}}{3b}\frac{x_{c.g.}}{c}\right.$$
$$-\frac{2c^2(\tan\beta_0 - \tan\theta_0)}{3b^2}\left(-\frac{6cn_{l_y}\tan\beta_0}{b} - 2n_{l_x}\tan\beta_0\right.$$
$$-n_{l_x}\tan\theta_0 - \frac{6cn_{l_y}\tan\theta_0}{b} + \frac{8cn_{l_y}\tan\beta_0}{b}\frac{x_{c.g.}}{c}$$
$$+\frac{8cn_{l_y}\tan\theta_0}{b}\frac{x_{c.g.}}{c} + 4n_{l_x}\frac{z_{c.g.}}{c} + \frac{16cn_{l_y}}{b}\frac{z_{c.g.}}{c}$$
$$\left.\left.-\frac{24cn_{l_y}}{b}\frac{z_{c.g.}}{c}\frac{x_{c.g.}}{c}\right)\right] \tag{73}$$

r^* Derivative of Yaw Moment Coefficient: C_{nr}

If the vehicle undergoes a yawing motion, the damping-in-yaw coefficient can be calculated from

$$(C_n)_r = \frac{1}{q_\infty S(b/2)}\left[\iint x(\mathrm{d}\boldsymbol{F})_{y-r} - \iint y(\mathrm{d}\boldsymbol{F})_{x-r}\right] \quad (74)$$

Integrating this yields

$$\frac{\partial C_n}{\partial(rb/2V_\infty)} = \frac{-8c^3 n_{ly}\tan\beta_0}{3b^3 M_\infty}\left(6\frac{x_{c.g.}^2}{c^2} - 8\frac{x_{c.g.}}{c} + 3\right) - \frac{\rho_2}{\rho_\infty}\sqrt{\frac{T_2}{T_\infty}}\frac{1}{M_\infty}\left[\frac{\tan\theta_0}{3}\left(n_{lx} + \frac{3cn_{ly}}{b} - \frac{4cn_{ly}}{b}\frac{x_{c.g.}}{c}\right) + \frac{2c^2(\tan\beta_0 - \tan\theta_0)}{3b^2}\left(-3n_{lx} - \frac{12cn_{ly}}{b} + 4n_{lx}\frac{x_{c.g.}}{c} + \frac{32cn_{ly}}{b}\frac{x_{c.g.}}{c} - \frac{24cn_{ly}}{b}\frac{x_{c.g.}^2}{c^2}\right)\right] \quad (75)$$

Calculation of C_L and $C_{L\alpha}$

The work that is used to validate these results requires the computation of coefficients in the wind axes. These coefficients are related to the coefficients in the body axis system for $\alpha = 0$ as follows:

$$C_L = -C_Z \quad (76)$$

$$C_{L\alpha} = -C_{Z\alpha} + C_X \quad (77)$$

Hypersonic Limit

A criticism of piston theory is that it does not reduce to the correct limit as $M_\infty \to \infty$ and $\gamma \to 1$, as does oblique shock theory that reduces to the Newtonian result. However, in the present work, piston theory is being applied behind the oblique shock created by the caret-wing, and, as a result, the expressions for C_Z, C_X, and C_m do reduce to the correct limit. In fact, piston theory is not being used to calculate these three coefficients as is normally done when it is applied to the freestream flow. It is interesting to evaluate the hypersonic limit of the stability derivatives that are calculated with piston theory. In each derivative, there are terms from the integration over the upper surface that contain $(1/M_\infty)$. These terms drop out as $M_\infty \to \infty$, thus giving the result that at high Mach numbers for the vehicles with attached shock waves, the upper surface contribution is negligible. The terms on the lower surface contain $(\rho_2/\rho_\infty)\sqrt{(T_2/T_\infty)}(1/M_\infty)$. In the limit of $M_\infty \to \infty$, this term tends to the finite value of $\sqrt{[2\gamma \sin^2\beta_0/(\gamma - 1)]}$. Therefore, in the hypersonic limit, these derivatives are finite. If the further limit of $\gamma \to 1$ is taken, the derivatives are singular. However, as an engineering tool, these expressions are perfectly valid and indeed are good approximations to the stability derivatives; γ does not approach unity in most flow situations of interest.

Validation

The results of the present theory have been partially validated by comparison with the experimental results of Kipke.[11] Kipke measured the performance of several caret-wings with design Mach numbers of 6, 8, and 10 at flight Mach numbers from 7.9 to 15.5. We have compared C_L, $C_{L\alpha}$, C_m, and $C_{m\alpha}$ from Eqs. (76), (77), (34), and (44), with his results for wing number 2 (design Mach number of 8) flying at Mach 7.9 and Reynolds number 2.7×10^6. The results are summarized in Table 1. Agreement to within 8% is obtained for the on-design condition. The error listed for the experimental data is related to measuring the coefficients from the published graphs; no experimental error was indicated in the published reports. Using the theory developed by Hui[12] to calculate $C_{m\alpha}$ for this caret-wing yields the result -1.433, 15% larger than the experimental value of -1.687. This difference is attributed to the fact that Hui's formula only accounts for forces on the lower surface; inclusion of the upper surface would lead to a smaller value.

The present formulation has also been compared to Hui's[12] results for a Mach 17 caret-wing with wedge angle, $\theta_0 = 20$ deg. The values of C_{mq} and $C_{m\alpha}$ are compared in Figs. 3 and 4. As can be seen, agreement is fairly good. The well-known quadratic behavior of C_{mq} is duplicated very well. In these figures, the value of $x_{c.g.}/c$ is the location of the vehicle c.g. in Hui's axis system, which has an axis along the lower surface ridgeline. For the sake of comparison, the c.g. was forced to be on this ridgeline. Hui's theory ignores the small term associated with $z_{c.g.}$, but the piston theory formulation does not. With the c.g. on the lower surface ridgeline, the two theories are calculating the same value. The piston theory coefficient

Table 1 Comparison of linear piston theory and Kipke experimental results ($\alpha = 0$)

Coefficient	Experiment	Piston theory	Difference
C_L	0.065 ± 0.002	0.060	−8%
$C_{L\alpha}$[a]	0.886 ± 0.010	0.887	0%
C_m[b]	−0.124 ± 0.002	−0.117	6%
$C_{m\alpha}$[a,b]	−1.687 ± 0.031	−1.823	−8%

[a]Per radian.
[b]Moments are taken with the c.g. at the nosetip of the caret-wing.

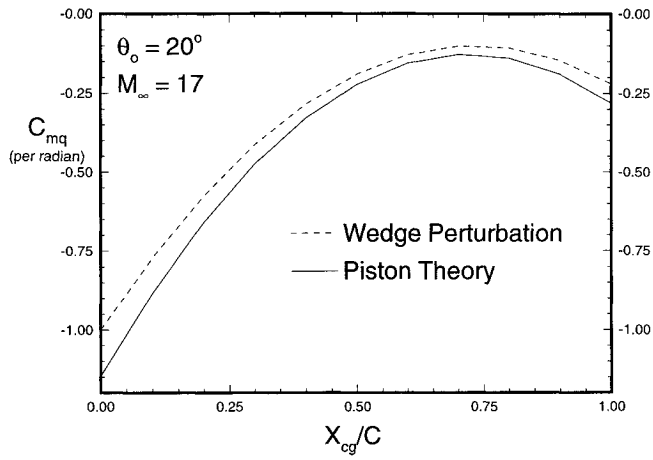

Fig. 3 C_{mq}, comparison of piston theory and Hui's wedge perturbation theory.

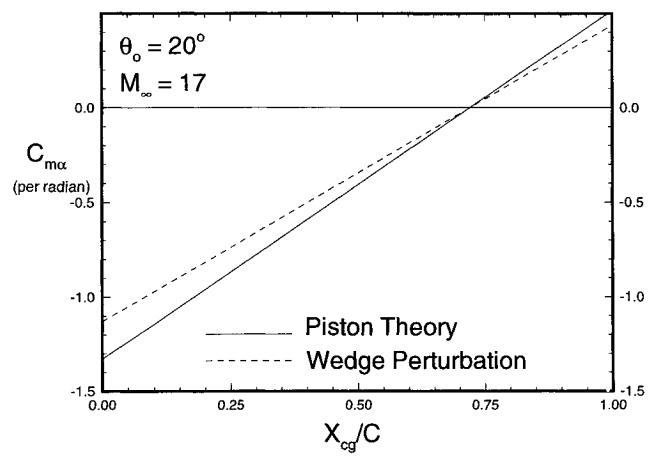

Fig. 4 $C_{m\alpha}$, comparison of piston theory and Hui's wedge perturbation theory.

was modified to exclude the upper surface, as does Hui, and conform to the nondimensionalization used by Hui. As expected, the piston theory overpredicts the pressure on the surface. Hui's theory includes the effects of reflected waves between the body and the bow shocks that weaken the pressure field. Hui compared his theory to experimental work by Pugh and Woodgate[13] for low Mach numbers (1.75 and 2.47) and found good agreement.

Off-Design Calculation

The previous results are for a caret-wing that is flying at its design Mach number. When the caret-wing is flying at off-design conditions, the flow is no longer completely two dimensional. If the flight Mach number is lower than the design Mach number, the shock moves away from the body, but stays attached to the leading edge. If the Mach number is greater, the shock moves toward the body as shown in Fig. 5. For the case of a flight Mach number greater than the design Mach number, we make the assumption that the flow stays two dimensional and that the turning angle of the flow continues to be the wedge angle of the on-design caret-wing. This assumption overpredicts the pressure on the outer portion of the caret-wing. The values predicted using this assumption are compared to Kipke's model 2 flying at higher Mach numbers in Figs. 6–9; agreement within 10% is achieved for most data points.

In Fig. 6 the value of the Newtonian limit for C_L has been plotted. The value of C_L predicted by the present work and the experimental data appear to be asymptotically approaching a higher value. This is not unexpected because $\gamma = 1.4$ for this flow. If only the high Mach number limit is applied to the expression for C_L for Kipke's wing 2, the expected limit

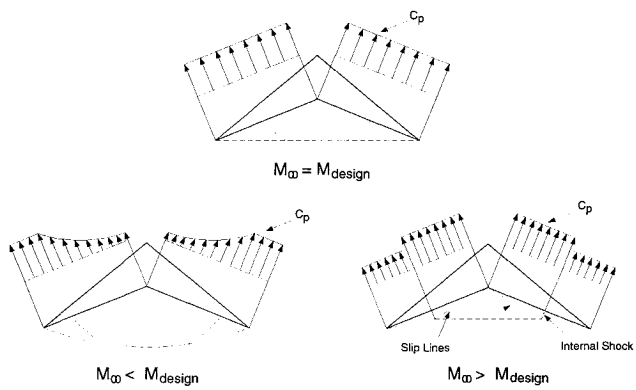

Fig. 5 Caret-wing shock structure, on- and off-design (after Ref. 11).

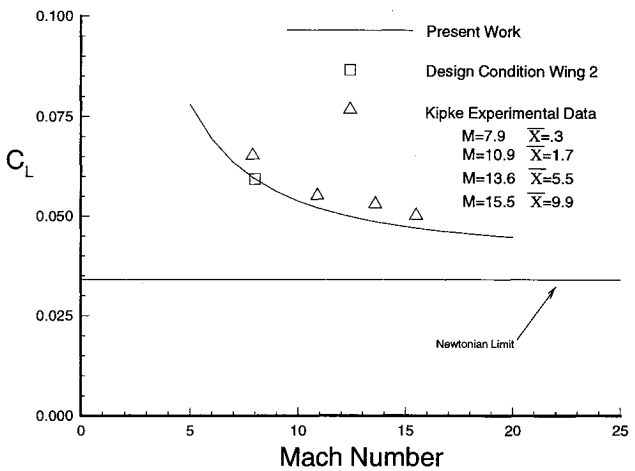

Fig. 6 C_L, comparison of Kipke experimental data and off-design calculation.

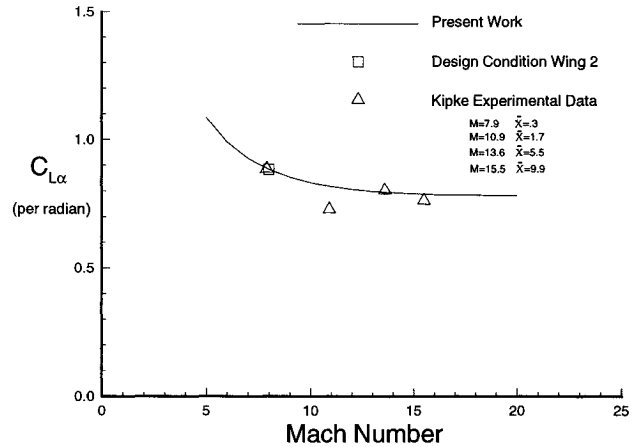

Fig. 7 $C_{L\alpha}$, comparison of Kipke experimental data and off-design calculation.

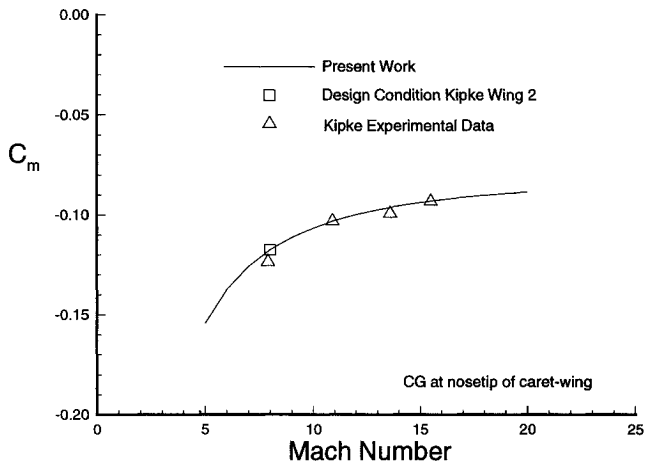

Fig. 8 C_m, comparison of Kipke experimental data and off-design calculation.

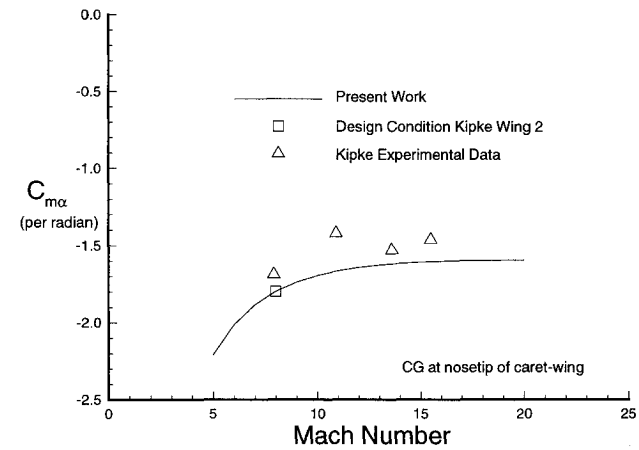

Fig. 9 $C_{m\alpha}$, comparison of Kipke experimental data and off-design calculation.

is 0.044, which corresponds to the present work and experimental data. As can be seen in Figs. 7 and 9, these coefficients approach a finite limit as Mach number increases as expected because $\gamma = 1.4$ for this flow.

Mach 6 Waverider Stability

As an example of the results obtained from the present theory, the coefficients have been calculated for a Mach 6 waverider with a wedge angle of 4.69 deg and are shown in

Table 2 Mach 6 waverider stability derivatives

Coefficient	Piston theory
C_Z	-0.037
$C_{Z\alpha}$	-0.792 rad^{-1}
C_{Zq}	0.190 rad^{-1}
C_X	-0.003
$C_{X\alpha}$	-0.043 rad^{-1}
L/D	12.2
C_m	0.009
$C_{m\alpha}$	0.190 rad^{-1}
C_{mq}	-0.449 rad^{-1}
$C_{Y\beta}$	-0.268 rad^{-1}
$C_{l\beta}$	0.191 rad^{-1}
$C_{n\beta}$	-0.079 rad^{-1}
C_{Yp}	0.191 rad^{-1}
C_{lp}	-0.229 rad^{-1}
C_{np}	-0.00035 rad^{-1}
C_{Yr}	-0.079 rad^{-1}
C_{lr}	-0.00035 rad^{-1}
C_{nr}	-0.176 rad^{-1}

Table 2. The c.g. location, given by Eq. (4), is behind the aerodynamic center that is at approximately $(x_{c.g.}/c) = \frac{2}{3}$. As a result, there is a nose-up pitching moment, and $C_{m\alpha}$ indicates a negative pitch stiffness. However, the damping-in-pitch coefficient C_{mq} is negative, and remains negative for all positions of $(x_{c.g.}/c)$. The effective dihedral $C_{l\beta}$ is positive as expected for a configuration with anhedral. The wing has negative yaw stiffness as can be seen from the negative value of $C_{n\beta}$. This is due to the fact the c.g. is placed so far back in the caret-wing.

Conclusions

Linear piston theory has been used to calculate the longitudinal and lateral stability derivatives for a caret-wing at hypersonic Mach numbers. The analysis has covered the on-design flight condition as well as flight Mach numbers above the design Mach number. Closed-form analytical expressions are given for the derivatives because of the simplicity of the caret-wing geometry. Comparison to previous analytical and experimental work done on longitudinal stability shows good agreement.

This work will be extended using numerical integration to waverider shapes with more complex geometries. It is suspected that the analytical sensitivities calculated from the closed-form expressions above can be used in doing optimization of these waverider shapes.

Acknowledgments

This work was supported by Research Grant NASA NCA-2-611. The authors would like to acknowledge their Contract Monitor Jeff Bowles at the NASA Ames Research Center for his support. Additionally we would like to acknowledge G. Hui and D. Liu who provided assistance and guidance at the start of this work.

References

[1]Bowcutt, K. G., "Optimization of Hypersonic Waveriders Derived from Cone Flows—Including Viscous Effects," Ph.D. Dissertation, Univ. of Maryland, College Park, MD, 1986.

[2]O'Neill, M. K. L., and Lewis, M. J., "Optimized Scramjet Integration on a Waverider," *Journal of Aircraft*, Vol. 29, No. 6, 1992, pp. 1114–1121.

[3]Takashima, N., and Lewis, M. J., "Navier-Stokes Computation of a Viscous Optimized Waverider," *Journal of Spacecraft and Rockets*, Vol. 31, No. 3, 1994, pp. 383–391.

[4]Jones, R. T., "Properties of Low-Aspect-Ratio Pointed Wings at Speeds Below and Above the Speed of Sound," NACA TN 1032, March 1946.

[5]Ribner, H. S., "The Stability Derivatives of Low-Aspect-Ratio Triangular Wings at Subsonic and Supersonic Speeds," NACA TN 1423, Sept. 1947.

[6]Polhamus, E. C., "A Concept of the Vortex Lift of Sharp-Edge Delta Wings Based on a Leading-Edge-Suction Analogy," NACA TN D-3767, 1966.

[7]Hui, G. W. H., "Aerodynamic Stability Theory of Hypersonic Wings," *Proceedings of the 1st International Hypersonic Waverider Symposium*, Dept. of Aerospace Engineering, Univ. of Maryland, College Park, MD, 1990.

[8]Liu, D. D., and Hui, W. H., "Oscillating Delta Wings with Attached Shock Waves," *AIAA Journal*, Vol. 15, No. 6, 1977, pp. 804–812.

[9]Lighthill, M. J., "Oscillating Airfoils at High Mach Number," *Journal of the Aeronautical Sciences*, Vol. 20, No. 6, 1953, pp. 402–406.

[10]Tarpley, C., and Lewis, M. J., "Stability Derivatives for Engine Integrated Waveriders with Viscous and Pitch Effects," AIAA Paper 94-0381, Jan. 1994.

[11]Kipke, K., "Experimental Investigations on Wave Riders (Caret Wings) in the Hypersonic Range," NASA TT F-12,115, 1969; Translation of "Experimentelle Untersuchungen an Wellenreiter-Flügeln im Hyperschallbereich," Deutsche Forschungsanstalt fuer Luft- und Raumfahrt, Brunswick Institure fuer Aerodynamik, Rept. 67/39 and DLR-FB-68-41, June 1968.

[12]Hui, W. H., "Stability of Oscillating Wedges and Caret Wings in Hypersonic and Supersonic Flows," *AIAA Journal*, Vol. 7, No. 8, 1969, pp. 1524–1530.

[13]Pugh, P. G., and Woodgate, L., "Measurements of Pitching-Moment Derivatives for Blunt-Nosed Aerofoils Oscillating in Two-Dimensional Supersonic Flow," Aeronautical Research Council, R&M 3315, 1963.